Annals of Microbiology (2019) 69:93–106
https://doi.org/10.1007/s13213-018-1406-3

ORIGINAL ARTICLE

Characterization of an extracellular polysaccharide produced by a Saharan bacterium *Paenibacillus tarimensis* REG 0201M

Nadia Boukhelata[1] · Farida Taguett[1] · Yahia Kaci[1]

Received: 1 June 2018 / Accepted: 8 November 2018 / Published online: 26 November 2018

Abstract

The purpose of this paper is to highlight the novel molecular characteristics and rheological properties of the polysaccharide produced by a bacterium isolated from extremophilic environment (Algerian Sahara). Phenotypic and molecular characteristics of the REG 0201M bacterial strain retained for this research were studied. Extracellular polysaccharide produced by REG 0201M was purified, characterized and its production was investigated. Analysis of 16S rDNA gene sequence showed that strain REG 0201M belonged to the species *Paenibacillus tarimensis*. In sucrose agar medium, 1.31 g dry weight of the polysaccharide per liter was produced. Evaluation of water absorption capacity showed that this polysaccharide was able to absorb 1000 times more water than its own weight. The average molecular weight determined by high-performance size exclusion chromatography multiangle laser light scattering was 1.718×10^6 g mol^{-1}. Analysis of the monosaccharide composition by high-performance anion exchange chromatography showed the presence of fructose (77.67%) as the main neutral sugar, followed by galactose (20.37%), arabinose (1.79%), and rhamnose (0.16%). Its global charge determined by the Zeta potential measurement was about -35.27 ± 0.66 mV. The main functional groups were elucidated by Fourier-Transform Infrared Spectroscopy while the surface morphology was resolved by scanning electron microscopy analysis. Moreover, the rheological data revealed shear thinning properties with the same general behavior of the studied polysaccharide compared to xanthan. These results show the great potential of this polysaccharide, which could help to promote its use in various industries by replacing synthetic polymers.

Keywords Rhizosphere · *Paenibacillus tarimensis* · Exopolysaccharide · Characterization · Rheology

Introduction

Exopolysaccharides (EPS) are extracellular metabolites produced by several microorganisms, such as bacteria, fungi, and blue-green algae (Trabelsi et al. 2018). EPS are complex polymers divided into two types: (i) homopolysaccharides (one type of repeating monosaccharide units) and (ii) heteropolysaccharides (repeating units constituting two to eight monosaccharides); in general, the repeating units are very regular, branched or unbranched and interconnected by glycosidic linkages. In addition, EPS can be soluble or insoluble in water, ionic, or non-ionic and contain a mixture of compounds (proteins, nucleic acids, pyruvic acid, O-methyl, O-acetyl, and sulfate groups) (Byrom 1987; Johns and Noor 1991).

These microbial EPS derived from natural and renewable resources have a wide range of environmental and industrial applications, because of their competitive advantages and possess particular features (biodegradability, biocompatibility and non-toxicity). Thus, a particular interest was undertaken to the discovery of a new bioactive EPS. Regarding their physiological role, EPS exhibit diverse functions including cell to-cell interactions, adhesion, and effective protection against extreme conditions as salinity and high or low temperature (Moshabaki Isfahani et al. 2018; Bajestani et al. 2017). In

Electronic supplementary material The online version of this article (https://doi.org/10.1007/s13213-018-1406-3) contains supplementary material, which is available to authorized users.

✉ Yahia Kaci
yahiakaci@yahoo.fr

Nadia Boukhelata
nanouboukhelata@yahoo.fr

Farida Taguett
ftaguett@usthb.dz

[1] Laboratory of Organism Physiology and Biology, Team of Soil Biology, Faculty of Biological Science, USTHB, BP 32, Algiers, EL Alia, Algeria

addition, due to their potential properties (viscosifying, emulsifying, pseudoplastic rheological behavior, and swelling capacity), they are used as bioflocculants, bioadsorbants, of heavy metals, drug delivery agents, anticoagulant, antioxidant, anti-inflammatory agent, antithrombotic, immuno-modulation and anticancer agent (Rani et al. 2018).

EPS of bacterial origin are being considered for bioprospecting by a lot of research groups all over the world. Today, a large number of *Paenibacillus* species isolated from diverse environments are known to produce a wide range of EPS (Raza et al. 2011; Liang and Wang 2015; Grady et al. 2016; Xu et al. 2016).

Despite the large molecular structure diversity of EPS produced by *Paenibacillus* spp., only two commercial EPS with known structures, i.e., levan and curdlan, have been described (Liang and Wang 2015). Thus, polysaccharides produced by *Paenibacillus* spp. can be considered as a very promising, unexplored source of microbial polysaccharides for the purpose of industrial application. To the best of our knowledge, very few studies have shown the structural and rheological characteristics of EPS produced by bacteria isolated from Saharan soil (Kaci et al. 2005; Taguett et al. 2015). At the time of writing, no information was available about EPS produced from *Paenibacillus tarimensis*.

Biomolecules from extremophilic bacteria are expected to possess unique characteristics (chemical composition and physico-chemical properties) which are useful in responding to the increasing demand of new active bioproducts (Gugliandolo et al., 2015).

In this context, the main goal of this research is to show the original properties of polysaccharides produced by bacteria isolated from extreme environments that have been little studied, such as the Saharan soils of Algeria.

Therefore, *P. tarimensis* REG 0201M bacterial strain is identified phenotypically and molecularly. Also, yield production, physico-chemical characteristics, molecular weight, monomer composition, and rheological properties of its extracellular polysaccharide are investigated.

Materials and methods

Selection and identification of bacterial strains

The bacterial strain REG 0201M was isolated from rhizospheric soil of durum wheat (*Triticum durum* L.), located in the Saharan region Reggane (south of Algeria. geographical coordinates: 26° 43′ N, 0° 09′ E). This bacterial strain was selected for its extensive production and viscosity (by touching with a sterile Pasteur pipette) of gel-forming EPS on Yeast Extract Sucrose Agar (YESA) medium. Initially, the morphological characterization of the isolated REG 0201 M was carried out. The Gram-reaction was examined by routine Gram staining method. The cell morphology, spore shape and position, sporangium swelling and cell motility were observed by photonic microscopy. The bacterial isolate was also examined for its biochemical and physiological characteristics such as: catalase and oxydase reactions; starch and casein hydrolysis; gelatin liquefaction, phosphorus solubilization; indole, methyl red and Voges-Proskauer tests; H_2S formation; and citrate utilization, according to standard procedures. Physiological tests, such as growth at different temperatures (20, 25, 30, 35, 40, 45, and 50 °C) and pH (2, 4, 6, 7, 8 and 10), were performed by culturing the strain in TSB broth (ZHBO CONDA) under the appropriate conditions.

The oxidation/fermentation of various carbon compounds was tested using microtiter plates (Bromothymol blue was used as a pH indicator). Plates were incubated for 24–48 h at 30 °C and the results were estimated by medium color change and culture growth.

Molecular identification of REG 0201M bacterial strain

The molecular identification of bacterial isolate REG 0201M by 16S rRNA complete genes sequencing was conducted at Biofidal-Themis laboratory (Vaulx-en-Velin, Lyon, France).

The 16S rRNA genes were amplified using the PCR primers 27f (5′-CAGAGTTTGATCCTGGCT-3′) and 1492r (5′-AGGAGGTGATCCAGCCGCA-3′) (Frank et al. 2008). The total PCR reaction mixture was carried out in a final volume of 20 μL which consisted of 4 μL of 5 × Mix HOT BIOAmp at 12.5 mM $MgCl_2$ reaction mixture, 1 μL of each primer (10 μM), 2 μL of 10 × GC-enhancer (Betaine at a final concentration of 1 M) and 1 μL of genomic DNA (2 ng).

The PCR program was conducted with activation of Mix HOT BIOAmp (96 °C for 12 min), then 35 cycles of denaturation (96 °C for 20 s), annealing (54 °C for 23 s), extension (72 °C for 2 min) and a final extension (72 °C for 10 min). The amplified PCR product was purified with ExoSap-It kit. The PCR products were sequenced by 96 capillaries ABI 3730XL DNA analyzer using BigDye V3.1 dye terminator kit (Thermo Fisher Scientific). Sequences were analyzed by CHROMAS Pro and compared with sequences available in GenBank (http://www.ncbi.nlm.nih.gov/BLAST) and PBIL (BIBI) (https://umr5558-bibiserv.univ-lyon1.fr/lebibi/lebibi.cgi). Multiple alignments with closer similarity sequences were analyzed using CLUSTAL W program, and the phylogenetic tree was constructed to predict the species-level characterization of the studied isolate through distance method based web-tool, according to the Neighbor-Joining algorithms using MEGA 6. Software.

EPS production and purification

EPS production was studied using the modified YEMA medium-containing sucrose (20 g L^{-1}) instead of mannitol. The YESA medium consisted of 0.4 g yeast extract L^{-1}, 20 g sucrose L^{-1}, 0.5 g K_2HPO_4 L^{-1}, 0.2 g $MgSO_4$ L^{-1}, 0.1 NaCl g L^{-1}, and 15 g agar L^{-1}. The pH was adjusted to 6.8 and the growth was carried out at 30 °C for 7 days.

The polysaccharide (EPS-R1) produced by REG 0201M was extracted from the culture dishes as described by Freitas et al. (2009). The culture broth was diluted with distilled water and centrifuged at 4 °C (6000 , 20 min) for cell separation. The supernatant was filtered through a serial membrane filter (Sartorius). The EPS in the cell and protein-free supernatant was precipitated by the addition of cold isopropanol at a ratio of 3:1 (*v*/*v*). The semi-purified EPS was further purified by dialysis using 1KD MWCO membrane (Spectra/Por 6 dialysis membrane pre-wetted RC Tubing-Spectrum Laboratories Inc., Rancho Dominguez, CA, USA) against deionized water over the course of 24 h. After dialysis, the polymer solutions were freeze-dried using a lyophilizer (Labconco Freeze Dry System 4.5 L, USA) and weighed.

Water absorption capacity and kinetic water loss of EPS-R1

The objective of this experiment was to evaluate the maximum amount of water retained by lyophilized EPS-R1. Thus, 2 mL of water was gradually added to 0.21 g of lyophilized EPS-R1 until saturation. The sample was incubated overnight to allow water enter the polysaccharide structure and to remove excess water. The sample was weighed and then dried at 105 °C, until complete water evaporation. WAC was calculated using the formula given by Ryuichiro and Nohata (1994):

$$\mathrm{WAC}\,(\%) = \frac{W_1 - W_0}{DW} \times 100$$

W_0 sample weight before absorption
W_1 sample weight after absorption
DW dried sample weight (where $DW = W_0$)

This experiment was also carried out to establish the kinetic water loss of EPS-R1 following thermal desiccation at 105 °C (using Sartorius thermo-balance). The weight of EPS-R1 was recorded every 2 min and then used to calculate *WL* of EPS-R1. Towards the end of the analysis, the moisture percentage (%) of EPS-R1 was calculated (the difference in sample weight prior to and following drying):

$$\mathrm{Moisture}\,(\%) = \frac{W_0 - W_1}{W_1} \times 100$$

W_0 weight of sample
W_1 weight of dry sample

Characterization of EPS-R1

Zeta potential (ζ)

The electrical charge (ζ-potential) of the used biopolymer (EPS-R1) was measured using particle electrophoresis instrument "Malvern instrument" (Nanosizer Instruments, USA). The ζ-potential was determined by measuring the direction and velocity of the particle motion in the applied electric field. The biopolymer was diluted to a concentration of about 10^{-4} g L^{-1} and the experiment was conducted at 25 °C.

The diluted solution was thoroughly mixed and then injected into the measuring chamber of the particle electrophoresis instrument. The ζ-potential measurements are reported as the average and standard deviation of measurements performed on three freshly prepared samples. ζ can be calculated in aqueous medium at moderate electrolyte concentration with the Smoluchowski equation (Smoluchowski 1916):

$$\xi = \eta\mu/\varepsilon$$

μ electrophoretic mobility
η viscosity
ε dielectric constant of the solvent

Scanning electron microscopy

The surface morphology of freeze-dried EPS-R1 was investigated by scanning electron microscopy (SEM); the images were obtained using SEM-EDX (Quanta 250).

FTIR analysis

The functional groups of EPS-R1 were analyzed using ATR-FTIR (Brucker Alpha-P). The spectrum was recorded over the range of wave numbers from 4000 to 400 cm^{-1} with a resolution of 2 cm^{-1}.

Molecular weight

The average molecular weights (M_n, M_w, M_z), the radius of gyration (R^2_g), and the polydispersity index of EPS-R1 were determined by high-performance size-exclusion chromatography multiangle laser light scattering (HPSEC-MALLS) as described by Rioux et al. (2007).

The HPSEC system consisted of a LKB Bromma 2150 HPLC-Pump (GE Healthcare Bio-Sciences Corp., Milford, USA), a 100-μL manual injecting loop and a Wyatt Optilab 903 refractometer (Wyatt Technology, Santa Barbara, USA).

The MALLS apparatus was equipped with a Wyatt Dawn-DSP laser photometer (Wyatt Technology, Santa Barbara, USA), a K5 flow cell and a He–Ne laser operating at λ = 632.8 nm.

Before measurement, the Dawn apparatus was standardized using Pullulan standard "P-50, Mw = 4.73×10^4 Da" (Shodex, Tokyo, Japan). Two columns were used in line: TSK-G6000 PW (7.5 mm × 300 mm) and a TSK-G3000 PWXL (6 μm, 7.8 mm × 300 mm) (Tosoh Bioscience, Tokyo, Japan). EPS-R1 (1.452×10^{-4} g) was dispersed in the mobile phase (0.1 M $NaNO_3$–0.02% NaN_3, filtered and degassed) to reach a concentration of 2%, then filtered through 0.45 μm filters (Chromspec Syringe Filters 13 mm PVDF, non-sterile). The flow rate was 0.4 mL min^{-1}; the analysis was performed at room temperature while the EPS sample was analyzed at 40 °C.

RI detector and MALLS data were analyzed using ASTRA software version 4.70.07 (Wyatt Technology Corp, Santa Barbara. CA). *Mw* was estimated using (*dn/dc*) = 0.146. The average molecular weights (M_w), the polydispersity index (M_w/M_n), and the radius gyration R^2_g were estimated using second-order Debye model.

EPS monosaccharide composition

Into a glass tube containing about 4 mg of EPS-R1, was added a solution containing trifluoroacetic acid (TFA) (1 mL, 2 N) and 1.05 g inositol L^{-1} as internal standard. The mixture was vortexed and placed at 100 °C for 1 h. The hydrolyzed solution was cooled, and then neutralized with barium carbonate under vigorous stirring. The released monomers were determined using high performance anion exchange chromatography (HPAEC) with pulsed amperometric detection (PAD) on a Dionex ICS 3000 system equipped with a CarboPAC PA1 column (4 mm × 250 mm). The hydrolyzate solutions were passed through a 0.22-μm syringe filter for HPLC analysis. The elution of neutral monosaccharides occurs isocratically with 18 mM NaOH at a flow rate of 0.7 mL min^{-1} and elution of uronic acids with an NaOH/NaOAc gradient (18 mM/0–0.5 M). Sugar identification was done by comparison with reference sugars (glucose, mannose, galactose, arabinose, rhamnose, xylose, fructose, fucose, glucuronic, and galacturonic acids); inositol was added as an internal standard (Taguett et al. 2015).

Rheological properties

Lyophilized EPS-R1 was dissolved in distilled water and rheological measurements were carried out on Rheometer ARES G2 (TA-Instrument, waters LLC, New Castle, Delaware, USA), equipped with a DIN concentric cylinders (the inner diameter of the Cup is 30 mm and the diameter of DIN Bob is 27.7 mm). The apparent viscosity was measured at 25 °C as function of shear-rate (1 s^{-1} to 1000 s^{-1}) for different EPS concentrations: 10^{-4} g L^{-1}, 5×10^{-2} g L^{-1}, 2.0 g L^{-1}, 4.0 g L^{-1}, and 8.0 g L^{-1}. All experiments were carried out in triplicates.

To compare the flow curves, data was fitted using the Cross model (Cross 1965) for high concentrations 2.0 g L^{-1}, 4.0 g L^{-1}, and 8.0 g L^{-1}, and Power law model (Ostwald and Auerbach 1926) for low concentrations 10^{-4} g L^{-1} and 5×10^{-2} g L^{-1}.

- Cross model:

$$\frac{\eta-\eta_\infty}{\eta_0-\eta_\infty} = \frac{1}{1+(\kappa\dot{\gamma})^n}$$

η viscosity at a given shear rate Σ
η_o viscosity at low shear rate
η_∞ infinite viscosity
k consistency
n power-law index

- Power-law model:

$$\sigma = \kappa\dot{\gamma}^n$$

σ shear stress at a given shear rate Σ
k consistency
n power-law index

Results and discussion

Phenotypic characteristics of REG 0201M bacterial strain

The phenotypic characterization of REG 0201M bacterial strain was carried out using the Bergey's Manual of Systematics of Archaea and Bacteria (De Vos et al. 2015). REG 0201M bacterial strain was gram-positive, the colonies were circular, smooth, opaque, and ivory pigmented on YESA plates. Cells were motile and presented rod shapes, occurring in single, pairs or short chains. Ellipsoidal endospores were formed in swollen sporangia. The tests were positive for catalase, oxidase, Voges–Proskauer reaction, hydrolysis of starch, casein and gelatin, but negative for nitrate reduction, indole, H_2S, urea and phosphorus solubilizing. Growth occurs at 20–40 °C; the optimum temperature was 25–35 °C. Cell growth was at pH 4–10; the optimum pH was 7. Acids were produced from adonitol, mannitol, glucose, rhamnose, sorbose, maltose, melibiose, sucrose, trehalose, melezitose,

raffinose, dextrin and starch. Details showing the general characters are summarized in Supplementary Table S1.

As shown in Supplementary Table S2, a large number of carbon sources were metabolized by the bacterial strain REG 0201M. The substrates used by this bacterium suggested its important adaptation capacities.

Molecular identification

The phylogenetic data obtained by comparing the complete 16S rDNA sequences of the bacterial strain REG 0201M (1482 bp, accession number FJ853212.2) and other bacteria from GenBank, showed the highest sequence similarity (99%) to *Paenibacillus tarimensis* SA-7-6 (Wang et al. 2008). The sequence similarities between *Paenibacillus tarimensis* strain REG 0201M and the other *Paenibacillus* strains were equal or less than 96% (Fig. 1). Agarose gel electrophoresis analysis of 16S rRNA genes amplified from the bacterial strain *Paenibacillus. tarimensis* REG 0201M is shown in Supplementary Fig. S1.

In order to demonstrate the differences between *P. tarimensis* SA-7-6^T and our isolate *P. tarimensis* REG 0201M, a comparative table containing the essential characteristics was established (Supplementary Table S3). Comparison of the main presented characters showed phenotypic differences among the two strains. *P. tarimensis* REG 0201M exhibited positive enzymatic activities such as oxidase and amylase, ability to ferment certain carbohydrates such as glycerol, fructose, rhamnose, and inositol, and grow at pH 5.7, unlike *P. tarimensis* SA-7-6^T (Table S3). These information allowed us to highlight the great adaptability of *P. tarimensis* REG 0201M under inhospitable conditions.

EPS production

In this part of study, we wanted to compare the yields of EPS production before and after purification. Wet EPS-R1 recovered directly from Petri dishes was weighed. The obtained data showed that *P. tarimensis* REG 0201M had the capacity to produce 29.10 g L^{-1} of EPS-R1. This latter was lyophilized and weighed to determine its estimated dry weight of 2.22 g L^{-1}. EPS-R1 (29.10 g L^{-1}) was purified, lyophilized and weighed. The resulting amount of EPS-R1 was estimated at 1.31 g L^{-1}. As previously stated by some authors, the amount of EPS produced by bacteria of different taxa may vary from 0.09 g L^{-1} to 6 g L^{-1}. The bacterial strain *Geobacillus* sp. 4004 was able to produce an EPS with yields of 90 mg L^{-1} (Nicolaus et al. 2002). The two polysaccharide-producing bacteria *Paenibacillus* sp. 1 V and *Paenibacillus sellifer* 7AII produced respectively 0.31 g L^{-1} and 1.05 g L^{-1} (Rättö et al. 2005). The amount of EPS from *Alteromonas macleodii* subsp. *fijiensis* reached 6 g L^{-1} (Raguénès et al. 1996). The same observations were made for the EPS-producing bacteria belonging to the genera *Lactobacillus* and *Propionibacterium*, widely used in dairy industries (Gamar et al. 1997). This means that the culture conditions could stimulate the production of EPS rather than bacterial growth. In response to the harsh environmental conditions (increased osmotic pressure of culture media, water stress), bacteria tend to protect themselves by producing large amounts of EPS; thus, forming a physico-chemical barrier against external changes (Gamar et al. 1997; Kilic and Dönmez 2008). On the other hand, comparison of the dry weight of EPS-R1 before and after purification did not show a big difference. It therefore appears that the crude EPS mainly contains polysaccharides.

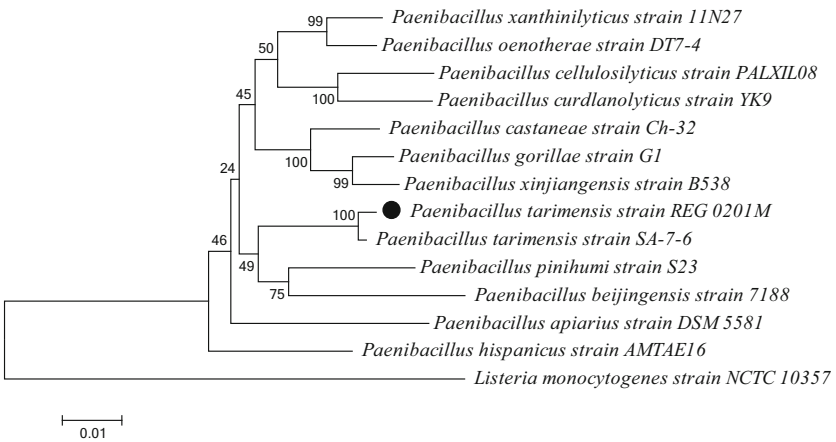

Fig. 1 The phylogenetic position of *Paenibacillus tarimensis* REG 0201M obtained with neighbor-joining method. The optimal tree with the sum of branch length = 0.37221527 is shown. The percentage of replicate trees in which the associated taxa clustered together in the bootstrap test (1000 replicates) is shown next to the branches. The tree is drawn to scale, with branch lengths in the same units as those of the evolutionary distances used to infer the phylogenetic tree. The evolutionary distances were computed using the maximum composite likelihood method and are in the units of the number of base substitutions per site. Evolutionary analyses were conducted in MEGA6. *Listeria monocytogenes* strain NCTC 10357 (NR044823.1) sequence was added as an out group for this tree

Table 1 Water absorption of some bacterial polysaccharides

Polysaccharides	WAC (%) per g of dried sample	References
SP	1349	Ryuichiro and Nohata (1994)
FP	1295.40	Ryuichiro and Nohata (1994)
bpS	432.65	Nazia and Nuzhat (2008)
bpG	426.50	Nazia and Nuzhat (2008)
bpF	422	Nazia and Nuzhat (2008)
Alginate	78.83	Nazia and Nuzhat (2008)
Cellulose	45.75	Nazia and Nuzhat (2008)
Xanthan	77	Nazia and Nuzhat (2008)
KYGB2	105	Kaci et al. (2005)
KYGT207	130	Kaci et al. (2005)
EPS-R1	1025	This study

Through these results, we found that the moisture content in crude EPS-R1 represented a very large proportion of their mass, estimated at 92.37%. Under the same conditions, Kaci et al. (2005) reported that EPS KYGT207 and EPS KYGB2 had a relative humidity of 97.3% and 95.9%, respectively.

Water absorption capacity and water loss kinetic of EPS-R1

The water absorption capacity of crude EPS-R1 revealed that the biopolymer absorbed 1000 times more water than its own weight. Compared to other biopolymers, EPS-R1 can be considered more water absorbing than others, such as cellulose, xanthan and alginate gum (used in industries) with *WAC* reaching 78.83, 45.75, and 77.0, respectively (Table 1). Likewise, other biopolymers such as EPS produced by *Alcaligenes latus* (SP and FP) can absorb up to 1000 times more water than its own weight (Table 2). Nazia and Nuzhat (2008) reported that the polysaccharide produced by *Pseudomonas aeruginosa* strain CMG1421 had the capacity to absorb water 400 times more than its dry weight. Kaci et al. (2005) reported that EPS KYGT207 and KYGB2 produced by *Rhizobium* sp. and *Paenibacillus* sp., respectively, absorb 100 times more water than their own weight (Table 1).

The study of time-dependent drying kinetics of EPS-R1 gel, showed a progressive decrease in the amounts of water by EPS-R1 relative to the pure water taken as a control (Fig. 2). Figure 2 clearly shows different phases of kinetic water loss; two phases for EPS-R1, and one phase for the control. To explain the differences between these phases, the speed of water evaporation (*S*) was calculated from the slopes of the corresponding curves $\left(\frac{\Delta WL}{\Delta T}\right)$. The results are summarized in Table 2.

In brief, we mention the following:

- The first phase (0–44 min): represents rapid evaporation due to high temperature (105 °C) and weak hydrogen bonds between water molecules and EPS. The amount of water lost during this phase was 74.70%. At 38 min, pure water (control) was totally evaporated.
- The second phase (44–96 min): characterized by a decrease in evaporation rate, which reflects the presence of a strong bonding involved in water retention. The amount of water lost during this phase was 86.74%. The amount of water lost at 96 min was 100%.

It appears that the amount of water loss, observed in this work, were lower than those given by other researchers. Kaci et al. (2005) reported that during the first phase of water evaporation, EPS KYEGB2 (produced by *Paenibacillus* sp.) and

Table 2 Parameters of water loss kinetics for water and EPS-R1

	Water	EPS-R1	
Phases range (min)	[0–38]	[0–44]	[44–96]
Phases duration (min)	38	44	52
S (% min^{-1})	2.92	1.80	0.34
R^2	0.99	0.99	0.93

S speed of water evaporation, R^2 regression coefficient

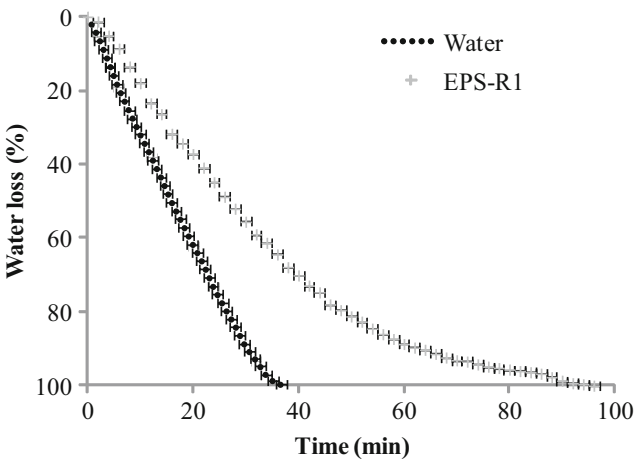

Fig. 2 Water loss kinetic of EPS-R1 sample after desiccation at 105 °C

EPS KYGT207 (produced by *Rhizobium* sp.) lost 85% and 70% of water, respectively, while EPS-R1 lost only 60.71%.

The calculated weight of EPS-R1 obtained at the end of the kinetic desiccation showed high moisture content (97.80%).

Therefore, EPS-R1 produced from *P. tarimensis* creates a microenvironment that can provide a buffered and predictable hydration phenomenon, especially under stressful conditions. Thus, EPS-R1 can represent an important source of water, especially in the arid and Saharan areas.

Characterization of EPS-R1

Zeta potential measurement (ζ)

The zeta potential measurement (ζ) showed a negatively charged value −35.27 ± 0.66 mV, indicating a highly charged EPS-R1 resulting from the presence of anionic groups in the polysaccharide chain. It should be noted that the average value of the zeta potential indicate the acidic character of the EPS. Many studies have shown considerable differences in the overall charge of bacterial EPS used in most industries (Table 3).

Scanning electron microscopic analysis of EPS-R1

This technique is considered as a powerful mean to study the surface morphology of polymers and could be used to clarify their physical properties (Han et al. 2015). As shown in Fig. 3, EPS-R1 appears as a compact matrix composed of thick filaments with irregular porosity (see arrow). It is important to note that there is no work allowing a comparison with the SEM micrograph of the EPS produced by the studied strain. The EPS structure could result in a higher water absorption/retention capacity, which is an attractive feature for a texturizing agent in the food industry (Han et al. 2015). The elemental composition of EPS-R1 was determined by SEM-EDX; the analysis revealed the presence of nine different elements (Fig. 3). We also noted the presence of carbon and oxygen as major components of EPS-R1, with 40.41% for the former and 41.96% for the latter. Other elements were also found in a relative proportion (K, Na, N, P, Cl, S, and Mg).

Table 3 Global charge of EPS produced by diverse bacteria

Bacteria	EPS	Charge	References
Pseudomonas aeruginosa	Alginate	Anionic	Öner (2013)
Gluconacetobacter xylinus	Cellulose	Neutral	Öner (2013)
Alcaligenes faecalis	Curdlan	Neutral	Öner (2013)
Leuconostoc mesenteroides	Dextran	Neutral	Öner (2013)
Sphingomonas paucimobilis	Gellan	Anionic	Öner (2013)
Pseudomonas aeruginosa	Hyaluronan	Anionic	Öner (2013)
Bacillus subtilis	Levan	Neutral	Öner (2013)
Xanthomonas campestris	Xanthan	Anionic	Öner (2013)
Paenibacillus tarimensis	EPS-R1	Anionic	In this study

FTIR spectra analyses

The functional moieties present in EPS-R1 were identified using FTIR spectroscopy (Fig. 4). The spectrum showed an intense broad peak at 3276.06 cm^{-1}, which indicated the presence of hydroxyl groups (Kavita et al. 2014). A minor band observed at 2926.30 cm^{-1}, well known to be typical of carbohydrates, indicated the presence of asymmetric C–H stretching vibration (Iyer et al. 2005). Furthermore, an asymmetric stretching peak was observed at 1625.42 cm^{-1}, showing the presence of stretching vibrations of carbonyl groups (C=O) in CONH moieties (Wang et al. 2013).

According to Freitas et al. (2009), the peak at 1625.42 cm^{-1} may correspond to ring stretching vibrations in mannose or galactose. The bands detected at 1416.32 cm^{-1} could be attributed to the symmetrical stretching of COO^{-} groups (Kavita et al. 2014). The peak at 1250 cm^{-1} band is due to C–O stretching vibrations in free carboxylic acids (San-Blas et al. 2012). Absorption peaks around 800 and 1200 cm^{-1} are characteristics of all sugar derivatives as well as β-glycosidic bonds between sugar monomers. The absorption peak at 1036.82 cm^{-1} is assigned to C–O–H, C–O–C, and C–O, indicating the presence of polysaccharides (Freitas et al. 2009; Wang et al. 2013; Nouha et al. 2016). The peaks at 811.77 and 773.57 cm^{-1} indicate the presence of α-glucosidic and β-glycosidic bonds (Ye et al. 2009). The small peaks observed at 559.11 and 623.55 cm^{-1} indicate the presence of glycosidic linkages present in the polysaccharide (Yu et al. 2016). The absorption peaks between 690 and 515 cm^{-1} correspond to stretching vibrations in alkyl-halide groups (Nouha et al. 2016).

The presence of those functional groups permits our polysaccharide to be used in a wide range of applications. The presence of hydroxyl (OH) and aliphatic (CH_2) groups makes the polysaccharide either water soluble or hydrophobic (Karbowiak et al. 2011). The hydrophilic and hydrophobic characters make EPS an appropriate emulsifier agent (Kavita et al. 2014) and/or a biosurfactant (Banat et al. 2010). The carboxylate functional group (COO^{-}) allow these polymers the ability to bind to other oppositely charged molecules, for example, heavy metals (Wei et al. 2011). Exopolymers can also play a role in preventing corrosion/erosion of metals owing to their anionic nature as well as their ability to chelate metals and ions (Donot et al. 2012).

Molecular weight

The average molecular weight (*Mw*) of EPS-R1 was measured and compared to pullulan P50, in this case used as a standard. The ratio $dn/dc = 0.146$ was used to calculate the molecular weight parameters; this was based on data obtained from High Performance Steric Exclusion Chromatography (HPSEC). The

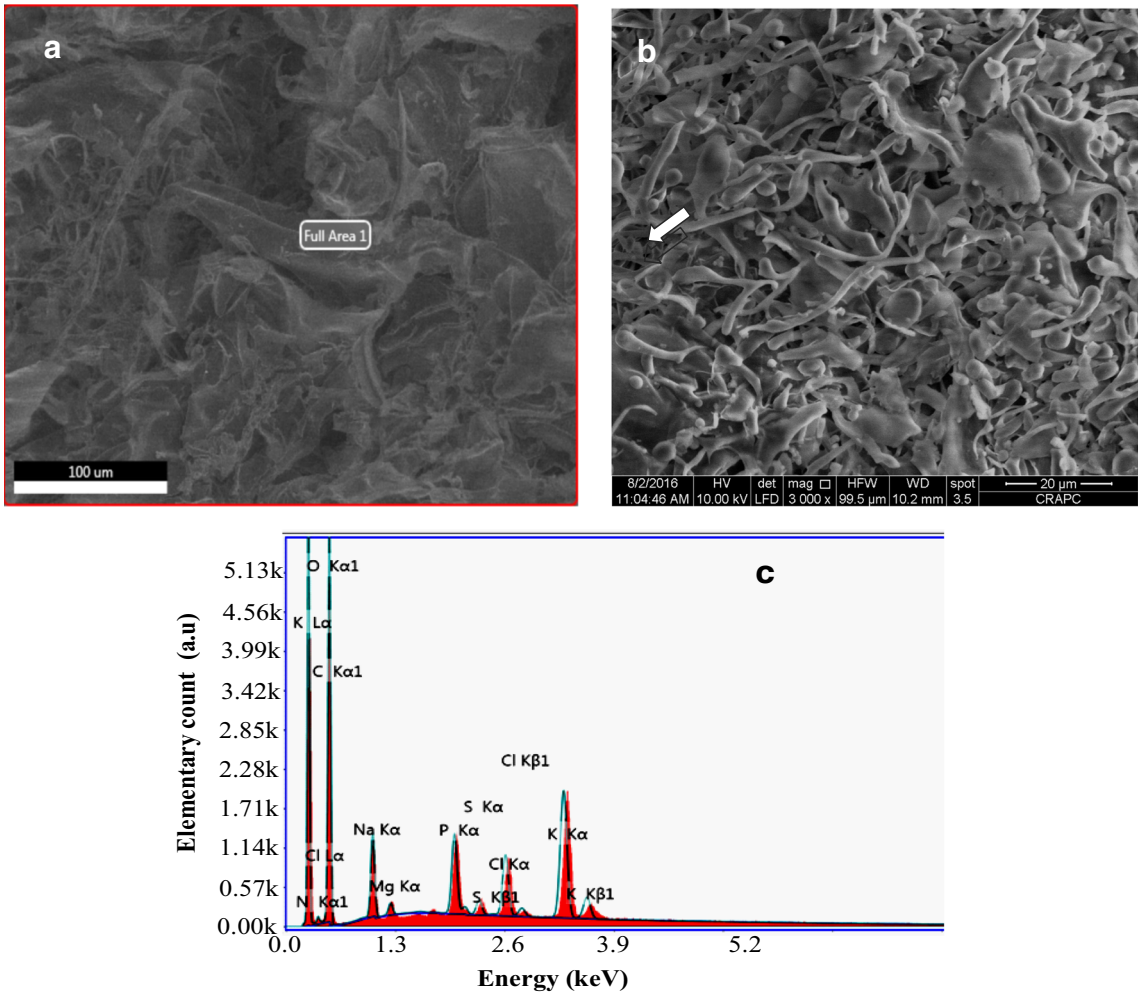

Fig. 3 Scanning electron micrographs of bacterial exopolysaccharide EPS-R1 with system at an accelerating voltage of **a** 20 kV and **b** 10 kV under image magnifications of **a** ×341 and **b** ×3000; **c** EDS spectrum of EPS-R1 obtained with full area

results revealed that the *Mw* of EPS-R1 (1.718×10^6 g mol^{-1}) was greater than the standard P50 pullulan (4.797×10^4 g mol^{-1}).

It has been reported that the average *Mw* of EPS, produced by *Paenibacillus* spp., varies between hundreds and thousands of kDa, depending on the culture strain, pH, temperature, initial carbon source concentration, culture techniques, and C/N ratio (Armstrong and Johns 1997; Liang and Wang 2015). Furthermore, sucrose-containing medium prompts bacteria to produce high-molecular-weight EPS (Liu et al. 2009).

With reference to other work, the *Mw* value of EPS-R1 was superior to other EPS produced by bacterial species *Paenibacillus* spp.; glucan, synthesized by the strain *P. polymyxa* JB115, has a *Mw* of 5.762×10^5 g mol^{-1} (Jung et al. 2007). Curdlan, produced by the strain *P. polymyxa* ATCC 21830, has a *Mw* of 1.7×10^5 g mol^{-1} (Rafigh et al. 2014). The *Mw* of EPS produced by *P. polymyxa* SQR-21 strain was estimated at 8.96×10^5 g mol^{-1} (Raza et al. 2011). Recently, we recorded an isolate from new bacterium *Paenibacillus bovis* sp. nov BD3526, which produced high molecular weight levan exceeding 2.6×10^6 g mol^{-1} (Xu et al. 2016). Evaluation of the molecular weight distribution (polydispersity index) for EPS-R1 revealed a value of 1.398 ± 0.109. This shows that our sugar molecules are evenly dispersed in an aqueous solution without formation of aggregates. This information is important because the functional properties of polysaccharides can be strongly influenced by the molecular weight distribution (Hwang et al. 2003). The value obtained is lower than that of glucan (polydispersity index: 5.81), synthesized by strain *P. polymyxa* JB115 (Jung et al. 2007), indicating a more homogeneous molecular weight distribution for EPS-R1 when compared to glucan. The gyration radius (R^2_g) of EPS-R1 was 85.50 nm, suggesting the presence of a large number of elementary units or monomers within the polysaccharide chain as well as a high degree of polymerization when compared to other polysaccharides such as xanthan (R^2_g: 70–90 nm) (Lee and Brant 2002).

Monosaccharide composition

The monosaccharide composition of EPS-R1 showed the presence of neutral fructose sugar as the main component (77.67%).

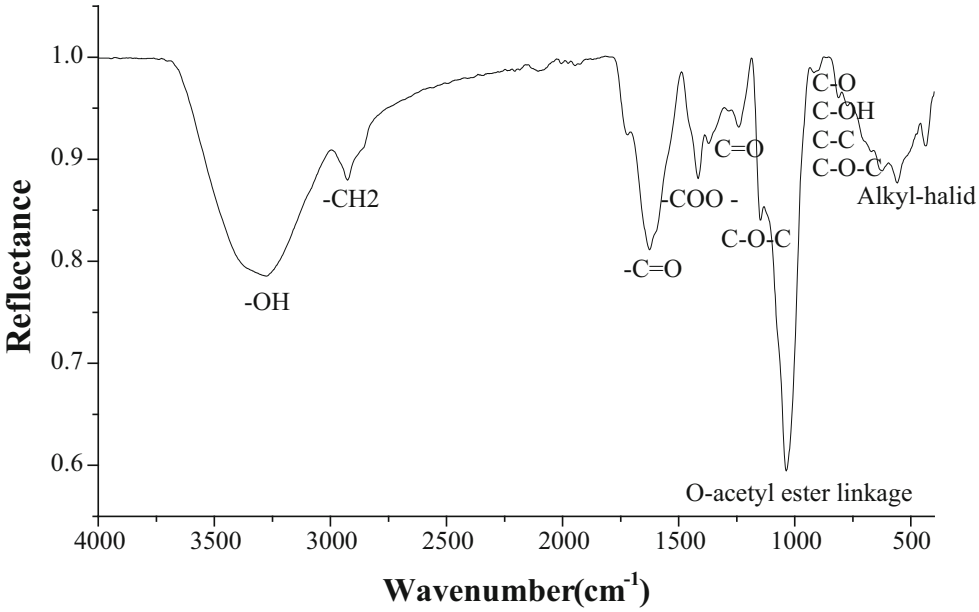

Fig. 4 ATR-FTIR of EPS-R1 in the range of 400–4000 cm^{-1}

EPS-R1 was also composed of other neutral sugars, with 20.37% of galactose, small amount of arabinose (1.79%) and traces of rhamnose (0.16%). Several authors have reported that the monosaccharide composition of EPS, produced by *Paenibacillus* spp., is usually composed of glucose, mannose, galactose, and glucuronic acid in various ratios (Table 4). On the other hand, a wide variety of EPS-producing *Paenibacillus* exist, depending on the type of *Paenibacillus* species, culture conditions, and the composition of the medium (Liang and Wang 2015).

These variations reveal the specificity of each strain for the production of EPS and, therefore, the increase in bioactive EPS which is known to replace synthetic chemicals which can have many side effects (Kenyon et al. 2005; Janczarek et al. 2009).

Rheology measurement

Figure 5 represents the different rheograms of EPS-R1 and xanthan (standard) at increasing concentrations (10^{-4} g L^{-1}, 5×10^{-2} g L^{-1}, 2.0 g L^{-1}, 4.0 g L^{-1}, and 8.0 g L^{-1}). The viscosity is determined at zero shear rate by the cross and power-law models. Rheological profiles showed that the apparent viscosity decreased with increasing the shear rate, indicating that EPS-R1 exhibited a character of non-Newtonian fluids with typical shear-thinning properties (Fig. 5a–e). According to Berwanger et al. (2007), this behavior is expected in polymer solutions of microbial polysaccharides. Han et al. (2015) reported that this property is important for various food processing procedures (mixing, pouring, and pumping) where different operating shear rates are applied.

Comparing the apparent viscosity at a zero shear rate (Fig. 4a–c), xanthan showed a higher viscosity at high concentrations (8.0 g L^{-1}, 4.0 g L^{-1}, and 2.0 g L^{-1}) than EPS-R1. According to Lai et al. (Lai et al. 2000), high EPS concentration prompts a more frequent molecular collision; thus, increasing the chances of more molecules coming in contact with each other. Moreover, we noted that at 2.0 g L^{-1} concentration, EPS-R1 was found to be less viscous compared to xanthan. According to literature (Sutherland 1994; Calero

Table 4 Chemical structures of EPS from *Paenibacillus* spp.

Paenibacillus species	EPS chemical composition	References
Paenibacillus sp. TKU023	Glucose and maltose	Liang and Wang 2015
P. polymyxa KCTC 8648P	Glucose, galactose, mannose, fucose, and glucuronic acid	Liang and Wang 2015
P. polymyxa NCIB 11429	Glucose, mannose, galactose, glucuronic acid, and pyruvate	Liang and Wang 2015
P. elgii B69	Glucose, glucuronic acid, xylose, and mannose	Liang and Wang 2015
Paenibacillus sp. 1 V	Rhamnose, glucose, galactose, mannose, and glucuronic acid	Rättö et al. 2005
Paenibacillus stillifer 7AII	Galactose, glucose, and mannose	Rättö et al. 2005
P. polymyxa EJS-3	Mannose, fructose, and glucose	Liang and Wang 2015
P. polymyxa SQR-21	Mannose, glucose, fructose, and glucuronic acid	Liang and Wang 2015
P. tarimensis REG 0201M	Fructose, galactose, arabinose, and rhamnose	This study

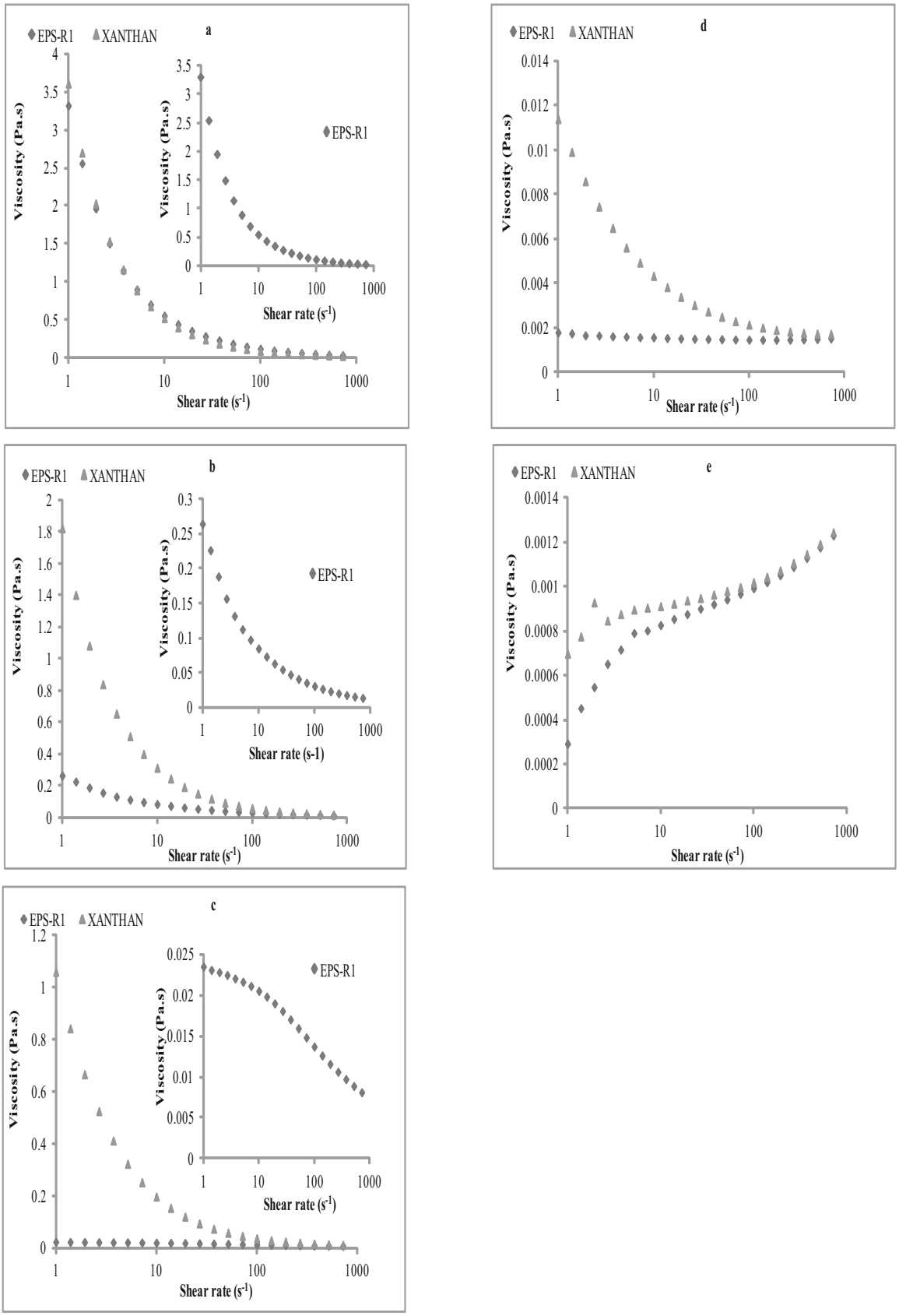

Fig. 5 Apparent viscosity as a function of shear rate of EPS-R1 and xanthan in aqueous solutions at concentrations of **a** 8.0 g L^{-1}, **b** 4.0 g L^{-1}, **c** 2.0 g L^{-1}, **d** 10^{-4} g L^{-1}, and **e** 5×10^{-2} g L^{-1}. The small pictures detail only the rheological curves of EPS-R1 at high concentrations

Table 5 Parameters of Cross model for EPS-R1at high concentrations

Samples	c (g L^{-1})	η_o (Pa.s)	η_∞ (Pa.s)	k (s)	n	R^2
EPS-R1	8.0	33,362.35 ± 31,147.42	0.013 ± 0.008	2,007,246.50 ± 2,579,417.35	0.688 ± 0.112	0.99
	4.0	1107.27 ± 1565.89	0.003 ± 0.000	5,770,000.00 ± 8,160,012.25	0.567 ± 0.072	0.99
	2.0	0.024 ± 0.004	0.004 ± 0.000	0.011 ± 0.0037	0.675 ± 0.005	0.99
Xanthan	8.0	53,116.8 ± 52,236.02	0.014 ± 0.001	152,823 ± 12,265.01	0.808 ± 0.005	0.99
	4.0	23,842.9 ± 156.23	0.006 ± 0.0002	246,331 ± 100.36	0.765 ± 0.001	0.99
	2.0	16.9093 ± 1.658	0.005 ± 0.0003	31.1106 ± 1.652	0.776 ± 0.001	0.99

c concentration; η viscosity at a given shear rate; η_o viscosity at low shear rate; n power-law index; η_∞ infinite viscosity; k consistency

et al. 2010), both shear rate and concentration of the polysaccharide in solution are known to directly affect the viscosity and degree of pseudoplasticity. Overall, for relatively concentrated polymer solutions, the increase in shear rate tends to change the order and orientation of the polymer chains towards the direction of the flowing fluid. This phenomenon causes a slippage between the chains and therefore a reduction in viscosity (Dunstan et al. 2004). At low shear rates, the polymer chains are entangled, resulting in a high viscosity solution. This behavior is dominant with all polymers present in solution, for example, xanthan, which is taken as reference in this study (Rinaudo and Milas 1982). According to Lapasin et al. (1995), the conformational changes reflect the presence of a large number of disordered macromolecules in solution, whereby the shapes appear to change continuously under the action of rotary motions.

At low EPS concentrations (10^{-4} g L^{-1}, 5×10^{-2} g L^{-1}), we noticed a change in trend. At 5×10^{-2} g L^{-1} concentration, the EPS-R1 solution exhibits a Newtonian behavior compared to xanthan (Fig. 5d). In a diluted system, Newtonian behavior is observed; the interactions between polymer chains are minimized while the size of macromolecules is extended to maximum capacity; the individual helices of the polymer are so distant that they have an insignificant influence on each other; thus, making their motion more facile (Xu et al. 2009). In contrast, it is well known that the viscosity of xanthan, even at low concentrations, is maintained when compared to other EPS (Paul et al. 1986). However, at 10^{-4} g L^{-1} concentrations, we noticed a surprising change in the behavior of EPS-R1 and xanthan within the shear-thickening fluid; the viscosity of the solution increased with increasing shear rate (Fig. 5e). This phenomenon could be attributed to the hydrogen bonding interactions between molecules causing an unusual viscoelastic response.

According to literature (Sochi 2010), this observation could also be due to the predominance of the "convergent-divergent geometry" extension existing in high-speed shear.

The results of the flow parameters obtained by the cross and power law viscosity models are summarized in Tables 5 and 6.

As stated by many authors, when the value of n is equal to 1, we notice the presence of a Newtonian fluid. Whereas, if the value of n is less than 1, we notice a pseudoplastic fluid. These values are representative of the different states of EPS-R1 solution at different concentrations (Xiu et al. 2011). The non-Newtonian behavior becomes important when the index n is less than 0.6 (Muller et al. 1994). Zhou et al. (2014), studied EPS-producing *Rhizobium radiobacter* S10, noted that the values of flow index (n), consistency coefficient (k), and viscosity are increased with increasing EPS concentration.

EPS-R1, with an elevated average Mw (1.7×10^6 g mol^{-1}) had a considerable viscosifying power at high concentration (8.0 g L^{-1}) when compared to xanthan, which is known for its high viscosity at high Mw (varying between 2 and 12×10^6 g mol^{-1}) (Paul et al. 1986). These results are in line with other studies showing that the EPS viscosity is strongly dependent on the average molecular weight (Han et al. 2015). According to Ebagninin et al. (2009), polymers with molecular weights between 10^5 g mol^{-1} and 10^6 g mol^{-1}, have a perfect correlation with the cross model.

The difference in the rheological properties of EPS is therefore a response of bacteria to protect themselves against external environmental conditions via enabling more water retention; thus, preventing sudden water evaporation (Amellal et al. 1998).

Through the rheological study, we have shown that EPS-R1 has interesting rheological properties, comparable to xanthan.

This lead us to reflect on the possibility of using these polymers to improve the structure of sandy soils and, thus, to yield better cereal production in the desert regions. In previous work (Kaci et al. 2005; Guilherme et al. 2015), bacterial EPS have been shown to play a role in soil structuring, which can result in an improved water retention capacity.

Table 6 Parameters of Power low model for EPS-R1 at low concentrations

Samples	c (g L^{-1})	η (Pa.s)	n	R^2
EPS-R1	5×10^{-2}	0.0010 ± 0.00015	1.043 ± 0.017	0.99
	10^{-4}	0.0005 ± 9.404 × 10^{-6}	1.131 ± 0.002	0.99
Xanthan	5×10^{-2}	0.0003 ± 0.0001	0.9312 ± 0.005	0.99
	10^{-4}	0.0006 ± 0.0002	1.1233 ± 0.006	0.99

c concentration; η viscosity at a given shear rate; n power-law index; R^2 correlation coefficient

Conclusion

The EPS-producing bacteria isolate from Algerian Sahara was identified and characterized as *P. tarimensis* REG 0201M. Outside the high EPS production, this bacterium with great physiological characteristics could be an excellent source for many applications in the future. In this study, for the first time, we have described an exopolysaccharide produced by *Paenibacillus tarimensis*. Thereby, the structural and rheological characterization of polysaccharide from *P. tarimensis* REG 0201M strain was investigated. EPS-R1 produced by this bacterium has shown that it can absorb 3 to 5 times more water than other biopolymers frequently used in various industries. So, this polymer can be used to enhance the production of plant species in drought-prone environments as well as in the area of regenerative medicine and cosmetic industry. EPS-R1 showed high molecular weight (1.718×10^6 g mol^{-1}) with narrow polydispersity index (1.39). The preliminary analysis of EPS-R1 reflected a new composition of this acidic heteropolymer. The functional groups of EPS-R1 identified by the FTIR spectrum have shown the presence of hydroxyl and aliphatic groups allowing its use as an emulsifier and/or a biosurfactant. Additionally, the presence of carboxylic groups allows it to participate in the bioremediation of terrestrial and aquatic environments via interacting with molecules of opposite charges such as heavy metal ions. The surface topography of the EPS-R1 analyzed by SEM revealed its fibrous and porous nature, while EDS showed the presence of various elements: C, O, K, Na, N, P, Cl, S, and Mg. The rheological behavior of EPS-R1 solutions exhibited an apparent shear-thinning character with exceptional viscosities in the low shear range, compared to the commercial benchmarks xanthan. These results indicate that EPS from *P. tarimensis* REG 0201M may be a new source of natural biopolymers useful for traditional biotechnological areas, such as food, cosmetic, pharmaceutical, and environmental applications.

Acknowledgments The authors are very grateful to Professor Sylvie Turgeon, Doctor Laurie-Eve Rioux and Diane Gagnon (Department of Food Science and Nutrition, Institute of Nutrition and Functional Food, Laval University, Quebec, Canada) for their valuable advice and technical assistance in Molecular weight determination and Rheological study of polysaccharides.

We would like to thank Claire Boisset (CNRS, CERMAV, Grenoble-France) for technical assistance in HPAEC-Dionex. We would like to thank Kamel Ait Messaoud and Okba Selama for providing language assistance.

Compliance with ethical standards

Conflicts of interest The authors declare that they have no conflict of interest.

Research involving human participants and/or animals N/A

Informed consent N/A

References

Amellal N, Burtin G, Bartoli F, Heulin T (1998) Colonization of wheat roots by an exopolysaccharide-producing *Pantoea agglomerans* strain and its effect on rhizosphere soil aggregation. Appl Environ Microbiol 64:3740–3747

Armstrong DC, Johns MR (1997) Culture conditions affect the molecular weight properties of hyaluronic acid produced by *Streptococcus zooepidemicus*. Appl Environ Microbiol 63:2759–2764

Bajestani MI, Mousavia SM, Jafarib A, Shojaosadati SA (2017) Biosynthesis and physicochemical characterization of a bacterial polysaccharide/polyamide blend, applied for microfluidics study in porous media. Int J Biol Macromol 96:100–110

Banat IM, Franzetti A, Gandolfi I, Bestetti G, Martinotti MG, Fracchia L, Smyth TJ, Marchant R (2010) Microbial biosurfactants production, applications and future potential. Appl Microbiol Biotechnol 87: 427–444

Berwanger AL, Da S, Scamparini ARP, Domingues NM, Vanzo LT, Treichel H, Padilha FF (2007) Produção de biopolímero sintetizado por *Sphingomonas capsulata* a partir de meios industriais. Ciênc Agrotecnol 31:177–183

Byrom D (1987) Polymer synthesis by micro-organisms: technology and economics. Trends Biotechnol 5:246–250

Calero N, Muñoz J, Ramírez P, Guerrero A (2010) Flow behaviour, linear viscoelasticity and surface properties of chitosan aqueous solutions. Food Hydrocoll 24:659–666

Cross MM (1965) Rheology of non-Newtonian fluids. A new flow equation for pseudo-plastic systems. J Colloid Sci 20:417–437

De Vos P, Ludwig W, Schleifer KH, Whitman WB (2015) Chapter introduction: "*Paenibacillaceae*" fam. nov. In: Whitman WB (ed) Bergey's manual of systematics of archaea and bacteria. John Wiley and Sons. https://doi.org/10.1002/9781118960608.fbm00114

Donot F, Fontana A, Baccou JC, Schorr-Galindo S (2012) Microbial exopolysaccharides: Main examples of synthesis, excretion, genetics and extraction. Carbohydr Polym 87:951–962

Dunstan DE, Hill EK, Wei Y (2004) Direct measurement of polymer segment orientation and distortion in shear: semi dilute solution behavior. Polymer 45:1261–1266

Ebagninin KW, Benchabane A, Bekkour K (2009) Rheological characterization of poly (ethylene oxide) solutions of different molecular weights. J Colloid Interface Sci 336:360–367

Frank JA, Reich CI, Sharma S, Weisbaum JS, Wilson BA, Olsen GJ (2008) Critical evaluation of two primers commonly used for amplification of bacterial 16S rRNA genes Appl. Environ Microbiol 74:2461–2470

Freitas F, Alves VD, Carvalheira M, Costa N, Oliveira R, Reis MA (2009) Emulsifying behaviour and rheological properties of the extracellular polysaccharide produced by *Pseudomonas oleovorans* grown on glycerol by product. Carbohydr Polym 78:549–556

Gamar L, Blondeau K, Simonet JM (1997) Physiological approach to extracellular polysaccharide production by *Lactobacillus rhamnosus* strain C83. J Appl Microbial 83:281–287

Grady EN, MacDonald J, Liu L, Richman A, Yuan ZC (2016) Current knowledge and perspectives of *Paenibacillus*: a review. Microb Cell Factories 15:203

Gugliandolo C, Spanò A, Maugeri TL, Poli A, Arena A, Nicolaus B (2015) Role of bacterial exopolysaccharides as agents in counteracting immune disorders induced by herpes virus. Microorganisms 3(3):464–483

Guilherme MR, Aouada FA, Fajardo AR, Martins AF, Paulino AT, Davi MFT, Rubira AF, Muniz EC (2015) Superabsorbent hydrogels based on polysaccharides for application in agriculture as soil conditioner and nutrient carrier: a review. Eur Polym J 72:365–385

Han Y, Liu E, Liu L, Zhang B, Wang Y, Gui M, Wu R, Li P (2015) Rheological, emulsifying and thermostability properties of two exopolysaccharides produced by *Bacillus amyloliquefaciens* LPL061. Carbohydr Polym 115:230–237

Hwang HJ, Kima SW, Choi JW, Yun JW (2003) Production and characterization of exopolysaccharides from submerged culture of *Phellinus linteus* KCTC 6190. Enzym Microb Technol 33:309–319

Iyer A, Mody K, Jha B (2005) Characterization of an exopolysaccharide produced by a marine *Enterobacter cloacae*. Indian J Exp Biol 43: 467–471

Janczarek M, Jaroszuk-S'ciseł J, Skorupska A (2009) Multiple copies of rosR and pssA genes enhance exopolysaccharide production, symbiotic competitiveness and clover nodulation in *Rhizobium leguminosarum* bv. *trifolii*. Antonie Van Leeuwenhoek 96:471–486

Johns MR, Noor E (1991) Recovery and purification of polysaccharides from microbial broth. Aust J Biotechnol 5:73–77

Jung HK, Hong JH, Park SC, Park BK, Nam DH, Kim SD (2007) Production and physicochemical characterization of β-glucan produced by *Paenibacillus polymyxa* JB115. Biotechnol Bioprocess Eng 12:713–719

Kaci Y, Heyraud A, Barakat M, Heulin T (2005) Isolation and identification of an EPS-producing *Rhizobium* strain from arid soil (Algeria): characterization of its EPS and the effect of inoculation on wheat rhizosphere soil structure. Res Microbiol 156:522–531

Karbowiak T, Ferret E, Debeaufort F, Voilley A, Cayot P (2011) Investigation of water transfer across thin layer biopolymer films by infrared spectroscopy. J Membr Sci 370:82–90

Kavita K, Singh VK, Mishraa A, Jha B (2014) Characterisation and anti-biofilm activity of extracellular polymeric substances from *Oceanobacillus iheyensis*. Carbohydr Polym 101:29–35

Kenyon WJ, Esch SW, Buller CS (2005) The curdlan-type exopolysaccharide produced by *Cellulomonas flavigena* KU forms part of an extracellular glycocalyx involved in cellulose degradation. Anton Leeuw 87:143–148

Kilic NK, Dönmez G (2008) Environmental conditions affecting exopolysaccharide production by *Pseudomonas aeruginosa*, *Micrococcus* sp., and *Ochrobactrum* sp. J Hazard Mat 154:1019–1024

Lai LS, Tung J, Lin PS (2000) Solution properties of hsian-tsao (Meaonaprocumbens) leaf gum. Food Hydrocoll 14:287–294

Lapasin R, De Lorenzi L, Pricl S, Torriano G (1995) Flow properties of hydrox-ypropyl guar gum and its long-chain hydrophobic derivatives. Carbohydr Polym 28:195–202

Lee HC, Brant DA (2002) Rheology of concentrated isotropic and anisotropic xanthan solutions. 1. A rodlike low molecular weight sample. Macromol 35:2212–2222

Liang TW, Wang SL (2015) Exopolysaccharides from *Paenibacillus* spp: production, isolation, structure, and bioactivities. Mar Drugs 13: 1847–1863

Liu J, Luo J, Ye H, Sun Y, Lu Z, Zeng X (2009) Production, characterization and antioxidant activities *in vitro* of exopolysaccharides from endophytic bacterium *Paenibacillus polymyxa* EJS-3. Carbohydr Polym 78:275–281

Moshabaki Isfahani F, Tahmourespour A, Hoodaji M, Ataabadi M, Mohammadi A (2018) Characterizing the new bacterial isolates of high yielding exopolysaccharides under hypersaline conditions. J Clean Prod 185:922–928

Muller FL, Pain JP, Villion P (1994) On the behaviour of non-Newtonian liquids in collinear ohmic heaters, In Proceedings of the 10th international heat transfer conference, freezing, melting, internal forces convection and heat exhchangers, vol. 4. Brighton, UK, p 285–290

Nazia J, Nuzhat A (2008) Production of biopolymers by *Pseudomonas aeruginosa* isolated from marine source. Braz Arch Biol Technol 51: 457–464

Nicolaus B, Lama L, Panico A, Schiano Moriello V, Romano I, Gambacorta A (2002) Production and characterization of exopolysaccharides excreted by thermophilic bacteria from shallow, marine hydrothermal vents of flegrean areas (Italy). Syst Appl Microbiol 25:319–325

Nouha K, Hoang NV, Tyagi RD (2016) Fourier transform infrared spectroscopy and liquid chromatography mass spectrometry study of extracellular polymer substances produced on secondary sludge fortified with crude glycerol. J Mat Sci Eng 5:3

Öner ET (2013) Chapter 2: microbial production of extracellular polysaccharides from biomass. In: Fang Z (ed) Pretreatment techniques for biofuels and biorefineries. p 35–56. https://doi.org/10.1007/978-3-642-32735-3_2

Ostwald W, Auerbach R (1926) The viscosity of colloidal solutions in the area of structure, laminar and turbulence. Kolloidn Zh 38:261–280

Paul F, Morin A, Monsan P (1986) Microbial polysaccharides with actual potential industrial applications. Biotech Adv 4:245–259

Rafigh SM, Yazdi AV, Vossoughi M, Safekordi AA, Ardjmand M (2014) Optimization of culture medium and modeling of curdlan production from *Paenibacillus polymyxa* by RSM and ANN. Int J Biol Macromol 70:463–473

Raguénès G, Pignet P, Gauthier G, Peres A, Christen R, Rougeaux H, Barbier G, Guezennec J (1996) Description of a new polymer-secreting bacterium from a deep-sea hydrothermal vent, *Alteromonas macleodii* subsp. *fijiensis*, and preliminary characterization of the polymer. Appl Environ Microbiol 62:67–73

Rani RP, Anandharaj M, Ravindran AD (2018) Characterization of a novel exopolysaccharide produced by *Lactobacillus gasseri* FR4 and demonstration of its in vitro biological properties. Int J Biol Macromol 109:772–783

Rättö M, Suihko ML, Siika-aho M (2005) Polysaccharide-producing bacteria isolated from paper machine slime deposits. J Ind Microbiol Biotechnol 32:109–114

Raza W, Makeen K, Wang Y, Xu Y, Qirong S (2011) Optimization, purification, characterization and antioxidant activity of an extracellular polysaccharide produced by *Paenibacillus polymyxa* SQR-21. Bioresour Technol 102:6095–6103

Rinaudo M, Milas M (1982) Xanthan properties in aqueous solution. Carbohydr Polym 2:264–269

Rioux LE, Turgeon SL, Beaulieu M (2007) Characterization of polysaccharides extracted from brown seaweeds. Carbohydr Polym 69: 530–537

Ryuichiro K, Nohata Y (1994) A new water absorbing polysaccharide from *Alcaligenes latus*. Biosci Biotechnol Biochem 58:235–238

San-Blas E, Cubillánb N, Guerrac M, Portillo E, Esteves I (2012) Characterization of *Xenorhabdus* and *Photorhabdus* bacteria by Fourier transform mid-infrared spectroscopy with attenuated total reflection (FT-IR/ATR). Spectrochim Acta A 93:58–62

Smoluchowski VM (1916) Theoretical observations on the viscosity of colloides. Kolloidn Zh 18:190–195

Sochi T (2010) Non-Newtonian flow in porous media. Polymer 51(22): 5007–5023

Sutherland IW (1994) Structure-function relationships in microbial exopolysaccharides, biotechnology advances. Biotechnol Adv 12: 393–448

Taguett F, Boisset C, Heyraud A, Buon L, Kaci Y (2015) Characterization and structure of the polysaccharide produced by *Pseudomonas fluorescens* strain TF7 isolated from an arid region of Algeria. C R Biol 338:335–342

Trabelsi I, Ktari N, Triki M, Bkhairia I, Ben Slima S, Sassi Aydi S, Aydi S, Abdeslam A, Ben Salah R (2018) Physicochemical, techno-functional, and antioxidant properties of a novel bacterial exopolysaccharide in cooked beef sausage. Int J Biol Macromol 111:11–18

Wang M, Yang M, Zhou G, Luo X, Zhang L, Tang Y, Fang C (2008) *Paenibacillus tarimensis* sp. nov., isolated from sand in Xinjiang, China. Int J Syst Evol Microbiol 58:2081–2085

Wang H, Ding S, Wang G, Xu X, Zhou G (2013) In situ characterization and analysis of *Salmonella* biofilm formation under meat processing environments using a combined microscopic and spectroscopic approach. Int J Food Microbiol 167:293–302

Wei X, Fang L, Cai P, Huang Q, Chen H, Liang W, Rong X (2011) Influence of extracellular polymeric substances (EPS) on Cd adsorption by bacteria. Environ Pollut 159(5):1369–1374

Xiu A, Zhou M, Zhu B, Wang S, Zhang J (2011) Rheological properties of Salecan as a new source of thickening agent. Food Hydrocoll 25: 1719–1725

Xu C, Willför S, Holmlund P, Holmbom B (2009) Rheological properties of water-soluble spruce O-acetyl galactoglucomannans. Carbohydr Polym 75:498–504

Xu X, Gao C, Liu Z, Wu J, Han J, Yan M, Wu Z (2016) Characterization of the levan produced by *Paenibacillus bovis* sp. nov BD3526 and its immunological activity. Carbohydr Polym 144:178–186

Ye L, Zhang J, Yang Y, Zhou S, Liu Y, Tang Q (2009) Structural characterization of a heteropolysaccharide by NMR spectra. Food Chem 112:962–966

Yu L, Xu S, Deng C, Li H, Yang Q, Xu Z, Chen J (2016) Preparation and partial structural characterization of the exopolysaccharide from *Bacillus mucilaginosus* SM-01. Carbohydr Polym 146:217–223

Zhou F, Wu Z, Chen C, Han J, Ai L, Guo B (2014) Exopolysaccharides produced by *Rhizobium radiobacter* S10 in whey and their rheological properties. Food Hydrocoll 36:362–368